Fig. 1 Laboratory setup of the single camera, marker based surgical navigation system

Methods

To evaluate if a system with the proposed physical dimensions can theoretically achieve the required accuracy a simulation of the imaging, the detection and the pose (position and orientation) estimation process is done. The simulation assumes that the camera lens is free of distortions. In the simulation predefined QR points in space (ground truth) are projected onto a virtual camera image plane. Due to the limited resolution of the virtual detector image the projected points are discretized on the image plane. The discretized projected points and the known points of the QR code form 2D–3D point correspondences. These point correspondences are used to recover the QR code pose by a Levenberg–Marquardt optimization [3]. In the system implementation the camera video stream is processed to perform a pose estimation based on detected QR code corner elements. Like in the simulation the pose is computed by setting up a 2D–3D point correspondence optimization problem and a Levenberg–Marquardt minimization. The corners of the QR code with known size and structure define the 3D points. The 2D points are the detected QR code corners in the camera image. For corner detection several preprocessing steps including a camera calibration and image undistortion, the detection of the QR code finder patterns and computation of the region of interest as well as a decoding of the QR code information for the QR code size are implemented. The main part of the algorithm detects the color of the pixel elements of the QR code (typically 21 × 21) to set up a corner matrix. The corner matrix is projected onto the image via a perspective projection according to the four known region of interest points. A subpixel refinement is performed for every point to detect its exact position. Finally, a validation of every point regarding the distance to its projected point and the pixel color around the point is performed to remove outliers. The accuracy of the pose estimation process is measured by comparing the computed QR code to camera transformation with the transformation measured with the 3D measurement system Optotrak.

Results

The simulation shows that the position and orientation of the QR code can be reconstructed with an RMS error between 0.01 mm/0.02° and 0.36 mm/0.31° depending on marker size (50 or 100 mm) and distance to the camera (100–200 mm). The measurement results of the implementation presenting the root mean square error are shown in Table 1. For the 100 mm × 100 mm QR code marker the RMS position error varies from 0.9 mm to 1.9 mm and the RMS orientation error varies from 0.2° to 0.6°. For the 50 mm × 50 mm QR code marker the RMS position error varies from 0.8 mm to 2.3 mm and the RMS orientation error varies from 0.3° to 2.3°. The main source of error in the system implementation is expected to be the camera calibration of the fisheye objective due to the strong fisheye distortion.

Table 1 Measured RMS translation errors Δx_{RMS}, Δy_{RMS}, Δz_{RMS} and RMS rotation errors $\Delta\alpha_{RMS}$, $\Delta\beta_{RMS}$, $\Delta\gamma_{RMS}$ for two different QR code sizes

QR code 100 × 100 mm			
Distance (mm)	100	150	200
Δx_{RMS} (mm)	1.5	1.7	1.5
Δy_{RMS} (mm)	1.3	1.9	1.5
Δz_{RMS} (mm)	1.0	1.2	0.9
$\Delta\alpha_{RMS}$ (°)	0.3	0.6	0.4
$\Delta\beta_{RMS}$ (°)	0.3	0.4	0.4
$\Delta\gamma_{RMS}$ (°)	0.2	0.4	0.2
QR code 50 × 50 mm			
Distance (mm)	100	150	200
Δx_{RMS} (mm)	1.5	1.6	1.4
Δy_{RMS} (mm)	1.2	1.9	1.7
Δz_{RMS} (mm)	0.8	1.6	2.3
$\Delta\alpha_{RMS}$ (°)	0.6	1.0	1.9
$\Delta\beta_{RMS}$ (°)	0.6	0.9	2.3
$\Delta\gamma_{RMS}$ (°)	0.3	0.5	0.6

A known systematic error was subtracted

Conclusion

The presented surgical navigation system has the advantage of a high level of integration, optimized line-of-sight between camera and marker and minimal hardware overhead. Simulations show that a sufficient precise pose estimation can be performed, assuming no camera distortions (error free camera calibration) and a good QR code marker detection. The accuracy of the implementation results can be sufficient in some case but need to be improved. The main error source is most likely due to the camera calibration of the fisheye objective.

References

[1] Peters TM (2006) Image-guidance for surgical procedures. Physics in medicine and biology 51(14): R505–R540.

[2] Kleemann M, Martens V, Hildebrand P, Beširević A, Schlichting S, Schweikard A, Bruch HP (2006) Die Erfassung des Raumes—Grundlagen der Trackingtechnologie. FOCUS MUL—Zeitschrift für Wissenschaft, Forschung und Lehre an der Universität zu Lübeck 4: 201–205.

[3] More JJ (1977) The Levenberg–Marquardt algorithm: Implementation and theory. Numerical Analysis Lecture Notes Math. 630: 105–116.

Image-guidance for laparoscopic liver ablations: technical evaluation in 54 patients

I. Paolucci[1], H. Nilsson[2], J. Freedman[2], D. Candinas[3], S. Weber[1], P. Tinguely[3]

[1]University of Bern, ARTORG Center for Biomedical Engineering Research, Bern, Switzerland [2]Danderyd Hospital, Karolinska Institutet, Division of Surgery, Department of Clinical Sciences, Stockholm, Sweden [3]University Hospital of Bern, Department of Visceral Surgery and Medicine, Bern, Switzerland

Keywords Image-guided surgery · Laparoscopy · Ablation · Liver

Purpose
Local ablation of liver tumors is an accepted tissue sparing treatment alternative for selected malignant liver lesions. Laparoscopy represents the minimal invasive treatment access of choice for lesions not amenable to percutaneous ablations and for combined treatments of resection and ablation. In laparoscopic liver tumor ablation, an ablation device (i.e. an ablation needle) has to be placed precisely into the tumor center. Conventionally, needle placement is performed under laparoscopic ultrasound (LUS) guidance and requires great experience, as the needle and the tumor have to be visualized together in a single image plane. Additionally, limited access for needle trajectories contribute to complexity of the procedure in a laparoscopic setting. Therefore, a stereotactic image-guidance system has been introduced to facilitate the treatment by providing additional guidance information during placement of the ablation needles.

Between January 2013 and October 2015, 346 lesions were treated using laparoscopic image-guided microwave ablation in 54 sessions. In the following retrospective analysis, the treatment approach was shown to be safe and effective in terms of low complication and local recurrence rates. From a technical point of view, several challenges related to the evaluation of accuracy when using the navigation technology were shown. To further accommodate the introduction of image-guidance in laparoscopic liver surgery, we here analyze the technical limitations and propose improvements, which will be the basis for future work in this domain.

Methods
For all treatments, the CAS-One Liver (CAScination AG, Bern, Switzerland) system was used for navigation and the Flex-800 (BK-Medical, Herlev, Denmark) LUS system for intraoperative visualization. An ablation device (Acculis MTA System, AngioDynamics, Latham, NY, USA) and a laparoscopic pointer were tracked by an optical tracking system (Polaris Vicra, Northern Digital, Ontario, Canada). The tip and the axis of both instruments were calibrated intraoperatively by aligning them with a calibration device. In each subject, a preoperative 3D model from computer tomography (CT) or magnetic resonance imaging (MRI) was obtained (MeVis Distant Service AG, Bremen, Germany) and intraoperatively registered using landmark based fiducial registration. For access of the pointer for registration, the round and falciform ligament were transected, whilst other mobilizations were avoided to reduce the change of the liver shape, thus avoid affecting the registration. After confirmation of the patient to image registration, a crosshair viewer aided for precise placement of the ablation device into the tumor (Fig. 1).

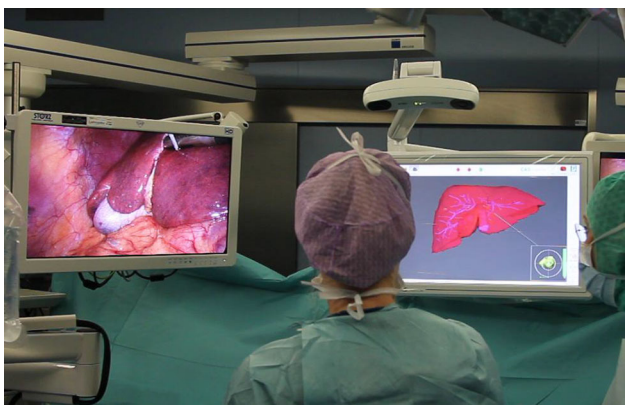

Fig. 1 Placement of the ablation device into the tumor guided with a cross hair viewer and a 3D scene on the image-guidance system

Postoperatively, accuracy and efficiency of the system were analyzed in each subject. Accuracy was assessed through existing intraoperative fiducial registration error (FRE) measurements together with a visual accuracy check of the registration. Efficiency was measured as the time needed for tool calibration and registration.

Results
The image-guided system was successfully applied in a total of 346 lesions during 54 cases of liver tumor ablation during laparoscopic surgery. A median of 2 registration attempts (range 1–10) were performed in each patient, and 4:38 min (range 0:26–19:34) were required per registration. The median operating time per subject was 102 min (range 31–420). The median time for tool calibration was 1:10 min (range 0:12–3:38). The median FRE was 7.9 mm (range 2.3–16.8). Overall, the time required for application of the image-guidance protocol (9:11 min) accounted for 9.3% of the time spent for surgery.

Conclusion
The applied image-guidance system and protocol were successfully applied without adding a significant delay (<10%) to the standard surgical time, thus representing an efficient treatment approach.

Even though the median fiducial registration error (FRE) is within a priori acceptable accuracy range (<10 mm) [1], the larger FRE range (<20 mm) indicated that sufficient registration accuracy could not be obtained in every case (8/54). This said, FRE is not a deterministic measure of registration accuracy, but indicates the likelihood of an insufficient registration accuracy [2], the FRE measurements may not be deemed fully adequate to assess the accuracy of the image-guided approach.

Thus, the accuracy of the intraoperative needle position could not be effectively assessed, mainly due to the lack of intraoperative pose estimation methods independent of the navigation. Consequently, we claim that more accurate intraoperative validation methods could be proposed, e.g. intraoperative 3D US, to measure target positioning error of the ablation device. Furthermore, the same modality could be used to assess ablation volumes intraoperatively for immediate evaluation of treatment success.

Finally, the time spent for tool calibration and registration were limited, and were likely compensated during the efficient targeting phase of the procedure. However, these steps introduce errors into the system and might reduce the surgeon's freedom regarding the manipulation of tissue. Therefore, we will focus on more registration-free guidance methods, and efficient intraoperative planning based on navigated laparoscopic ultrasound.

References

[1] Mahnken AH, Wilhelm KE, Ricke J, *CT- and MR-Guided Interventions in Radiology*. Springer, 2013.
[2] Fitzpatrick JM, "The role of registration in accurate surgical guidance.," *Proc. Inst. Mech. Eng. H.*, vol. 224, no. 5, pp. 607–22, 2010.

Novel methods for image guided surgical navigation using ToF scanner and optical IR tracking

M. Boyarkin[1], O. Egorov[1], K. Bychenkov[1], S. Chaplygin[2], A. Kolsanov[2]
[1]sMedX LLC, Samara, Russian Federation
[2]SamSMU, Samara, Russian Federation

Keywords Navigation system · Optical tracking · Image-guided surgery · Time of flight

Purpose
Modern IR-based image-guided surgery (IGS) navigation provides precise surgical navigation but has a number of limitations. For IR tracking a rigid infrared marker should be mounted on the patient, otherwise, frequent patient registration is required. Unfortunately, ToF based IGS navigation is not so efficient due to the technical